

X-ray Detectors I

Fundamentals

Sol M. Gruner

Physics Dept. & Cornell High Energy Synchrotron Source (CHESS)

Cornell University

Ithaca, NY 14853

smg26@cornell.edu



X-ray Detectors

Successful synchrotron science is dependent upon the presence of a succession of elements:

- (1) Synchrotron sources to generate the x-rays.
- (2) Beamline optics to deliver the x-rays to the specimens.
- (3) Specimens which can handle the dose.
- (4) Detectors which can collect the data, and
- (5) Procedures to analyze the data.

In this lecture we focus on detectors, which are both the orphans and the Achilles heel of synchrotron studies. The emphasis will be on the principles behind area detectors.



Lectures Outline

- Intro to photon counters & integrators
- General detector characteristics & evaluation
 - DQE & uncertainty
 - Spatial resolution, etc.
- Some photon counters in detail
 - Scintillator/phototube combinations
 - Gas counters
- Some integrating detectors in detail
 - Film
 - Image plates
 - CCD detectors
 - The quantum signal chain
 - Designing detectors
- Semiconductor Detectors
 - Si(Li) & Ge(Li)
 - Silicon drift detectors
 - Direct detection CCDs
 - Pixel Array Detectors (hybrids)



Counters vs. Integrators

Photon counters detect individual x-rays and store the counts in digital memory. **Integrators** analog sum the signal in some medium before digitizing. Both types can be photon counting statistic limited. Photon counters tend to be **count-rate limited** and integrators tend to be **duty-cycle limited**. Important types:

Photon Counters

1. Scintillator/phototube counters
2. Gas-filled wire counters
3. Si(Li) & Ge(Li) detectors
4. Silicon drift chambers
5. Digital Pixel Array Detectors (dPADs)

Integrators

1. Film
2. Storage phosphors
3. Phosphor-coupled imagers
 - a. Vidicon
 - b. Diode array
 - c. CCD
4. Direct detection CCDs
5. Analog Pixel Array Detectors (aPADs)



Characteristics and Metrics

- Detective Quantum Efficiency (DQE) & accuracy
- Spatial resolution
- Stopping power
- Dynamic range
- Energy resolution
- Practical considerations:
 - Nonlinearity
 - Reproducibility
 - Difficulty of calibration
 - Cost
 - Robustness
 - Formal & size
 - Ease of use

Useful references

Calibrations: Barna et al., *Rev Sci Instr* 70 (1999) 2927.

CCD Detector review: Gruner et al., *Rev Sci Instr* 73 (2002) 2815.



DQE

Detective Quantum Efficiency, DQE, an overall measure of the efficiency and noise performance of a detector :

$$DQE \equiv (S_o / N_o)^2 / (S_i / N_i)^2, \quad (1)$$

where S is signal, N is noise, o = output and i = input. DQE measures the degradation due to detection in the signal-to-noise ratio. For a signal source which obeys Poisson statistics,

$$S_i / N_i = S_i / \sqrt{S_i} = \sqrt{S_i}.$$

Ideal detector \Rightarrow no additional detector noise \Rightarrow preserving the incident signal-to-noise ratio, *i.e.*, $DQE = 1$. Real detectors always have $DQE < 1$ because of detector noise. DQE automatically accounts for input and output signals of a different nature (e.g., x-rays in, stored electrons out), since it is a ratio of dimensionless numbers.

DQE is a function of many variables, e.g.,

- Integrated dose
- X-ray spot size
- Duration of exposure
- Signal rate
- X-ray energy



General Features of the DQE

- A true set of DQE curves allow one to predict much about detector performance, but many (if not most) published DQE curves are fictions!
- The DQE is a function of many relevant variables. In area detectors, it is almost always dependent on the size of the integration area.
- All DQE curves exhibit a peaked form with lower DQE at low and high doses. Don't trust DQE's which do not.
- Low DQE at low dose is due to the competition between detector stopping power and noise vs. the signal per x-ray.
- Low DQE at high dose arises from signal dependent aberrations, e.g., saturation, signal-induced noise, etc.
- The goal is have the DQE approach 1 rapidly with dose and stay there over a wide dose range.



Example DQE Curves

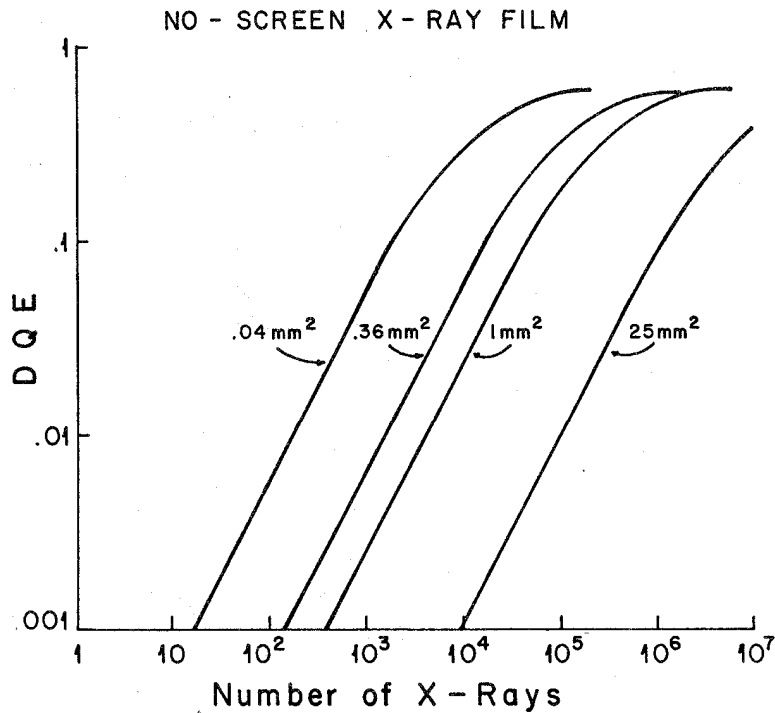


Figure 1 The detective quantum efficiency (DQE) of No-screen X-ray film for 8 keV X-rays. The number near each curve indicates the size of the integration area.

Gruner et al., IEEE Trans Nuc. Sci. NS-25 (1978)562

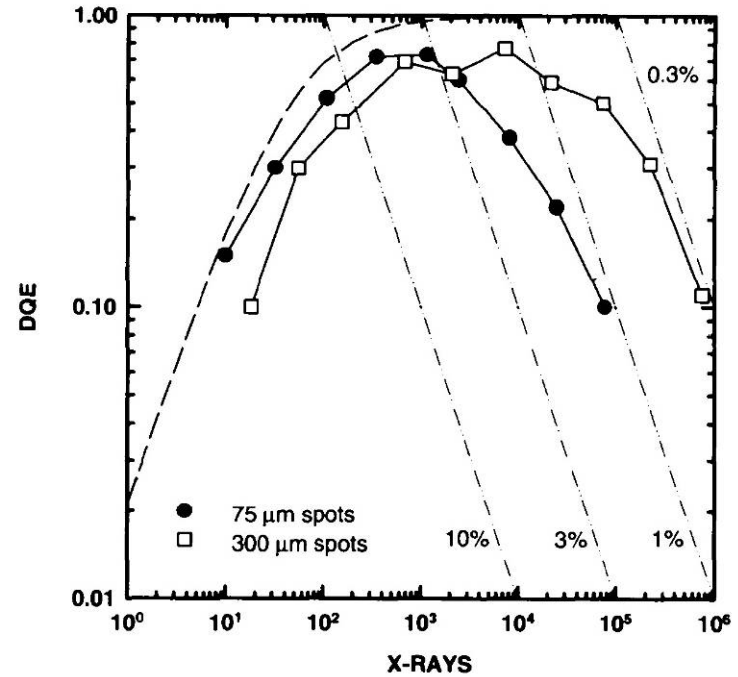


Fig. 3. DQE versus dose for 75 μm (●) and 300 μm (□) spot illumination from 8 keV X-rays. The integration area for the spots was a circle of radius 3.4 pixels (37 pixels in total in spot) for the 75 μm spots and a radius of 5.4 pixels (97 pixels in total in spot) for the 300 μm spots. As in Fig. 2, the fall-off in the DQE curve at low dose is caused by the read noise associated with each pixel. The dashed line indicates the expected DQE for a 37-pixel patch with a read noise of 1.1 X-ray photons pixel⁻¹. Fall-off at high dose is due to nonuniformities in sensitivity, on length scales of less than 2 pixels, that are not readily correctable (see text). The dash-dotted lines shown in the figure represent levels of accuracy (output noise per dose) for individual spot measurements.

Tate et al., J. Appl. Cryst. 28 (1995) 196



DQE ≤ 1

One reason DQEs are often erroneously high is because of a failure to appreciate the way in which poor detector resolution smooths flood-illumination. A common way to measure the DQE is to flood-illuminate the detector with a uniform x-ray source of known intensity. Many frames of nominally identical images are recorded so as to deliver an average of N x-rays/pixel/frame. The measured std deviation in a given pixel from all frames is used as the output noise and the mean recorded intensity is the output signal. Since the input dose/pixel is known, the input signal, N , and input noise, \sqrt{N} are both known, so the DQE can be calculated.

The problem is that this only works if the detector has ideal resolution. To see this, consider two detectors, both of which are ideal in that they contribute no detector noise. The first has ideal resolution and all the incident signal which falls onto a given pixel area contributes signal only to the corresponding output pixel. The second detector has finite resolution such that each incident x-ray contributes, for the sake of argument, uniformly to 4 pixels. Under identical illumination, both detectors will record the same avg signal/pixel. However, the noise/pixel in the first detector will go as \sqrt{N} . But the noise/pixel in the low resolution detector will go as $\sqrt{4N} = 2\sqrt{N}$, because each pixel has contributions from 4 times as many x-rays, so the image is less grainy. The detector is effectively smoothing the image. Unless the effect of resolution is taken into account, the apparent DQE per pixel of the low resolution detector will exceed 1!



DQE ≤ 1

Accounting for resolution in the DQE is more difficult with real detectors. The experimentally safest way is not to illuminate with a flood-field, but with x-ray spots, e.g., a flood-field through a shadow mask of holes of known size. It will be seen that the measured DQE falls as the spot size approaches the width of the point spread function.

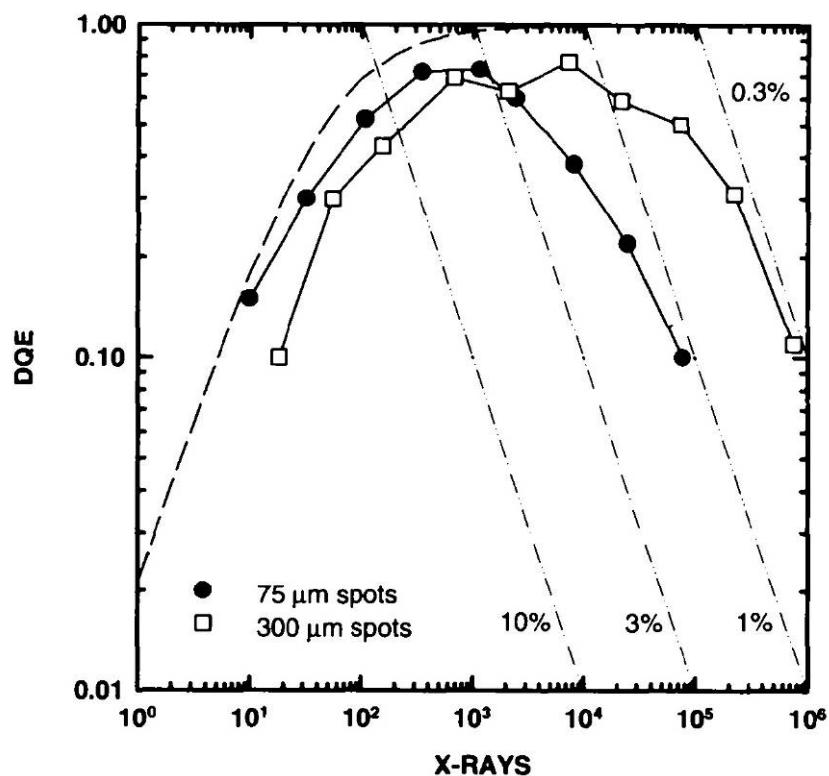


Fig. 3. DQE versus dose for 75 μm (\bullet) and 300 μm (\square) spot illumination from 8 keV X-rays. The integration area for the spots was a circle of radius 3.4 pixels (37 pixels in total in spot) for the 75 μm spots and a radius of 5.4 pixels (97 pixels in total in spot) for the 300 μm spots. As in Fig. 2, the fall-off in the DQE curve at low dose is caused by the read noise associated with each pixel. The dashed line indicates the expected DQE for a 37-pixel patch with a read noise of 1.1 X-ray photons pixel^{-1} . Fall-off at high dose is due to nonuniformities in sensitivity, on length scales of less than 2 pixels, that are not readily correctable (see text). The dash-dotted lines shown in the figure represent levels of accuracy (output noise per dose) for individual spot measurements.

Tate et al., J. Appl. Cryst. 28 (1995) 196



The Accuracy

Accounting for resolution in the DQE is more difficult with real detectors. The experimentally safest way is not to illuminate with a flood-field, but with x-ray spots, e.g., a flood-field through a shadow mask of holes of known size. It will be seen that the measured DQE falls as the spot size approaches the width of the point spread function.

The **Accuracy, ρ** , (also known as the uncertainty) measures the output noise relative to the signal, *i.e.*,

$$\rho = N_o/S_o.$$

Therefore, for a Poisson x-ray source

$$\rho = (N_i \times DQE)^{-1/2}. \quad (2)$$

Allows determination of # x-rays needed to measure a signal to a given accuracy with a detector of a given *DQE*. The accuracy for an ideal detector is $1/\sqrt{S_i}$, e.g., 100 x-rays are required to measure to 10% accuracy, and 10^4 x-rays are needed for a 1% accurate measurement. Nonideal detectors ($DQE < 1$) always require more x-rays than the ideal to measure to a given accuracy.



The Accuracy

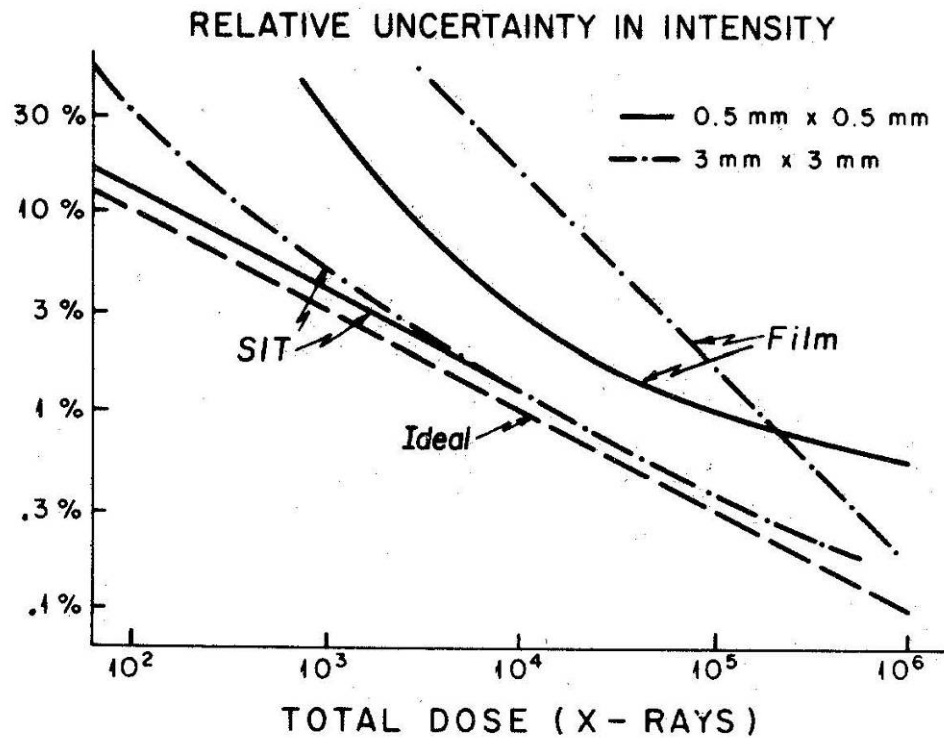


Fig. 2. The accuracy of the SIT vs. dose for two areas of integration. The accuracy of X-ray film and an ideal detector are graphed for comparison. Note that the speed advantage of the SIT relative to X-ray film is given by the ratio of doses needed to measure a signal to a given accuracy in a given area.

Gruner & Milch, Trans. ACA, 18(1982)149.



Detector Resolution

Spatial Resolution quantifies ability to independently measure adjacent signals:

- **Point Spread Function (PSF):** spread of intensity in the output image as a result of an incident point signal.
- **Line Spread Function**

$$LSF(x) = \int PSF(x, y) dy.$$

- **Modulation Transfer Function**

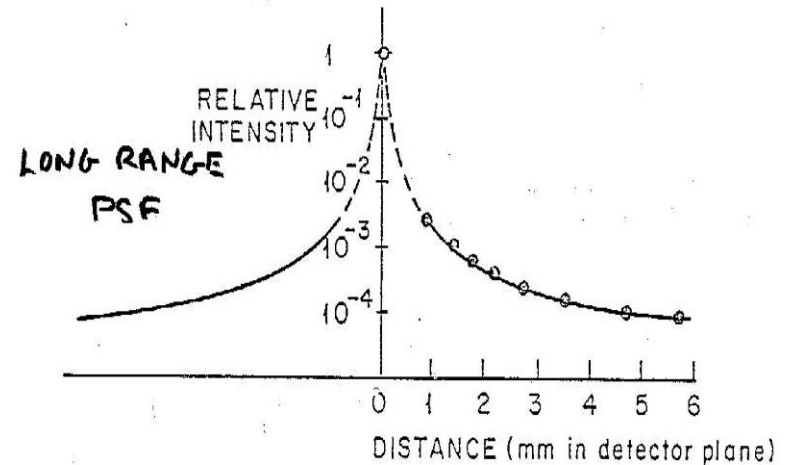
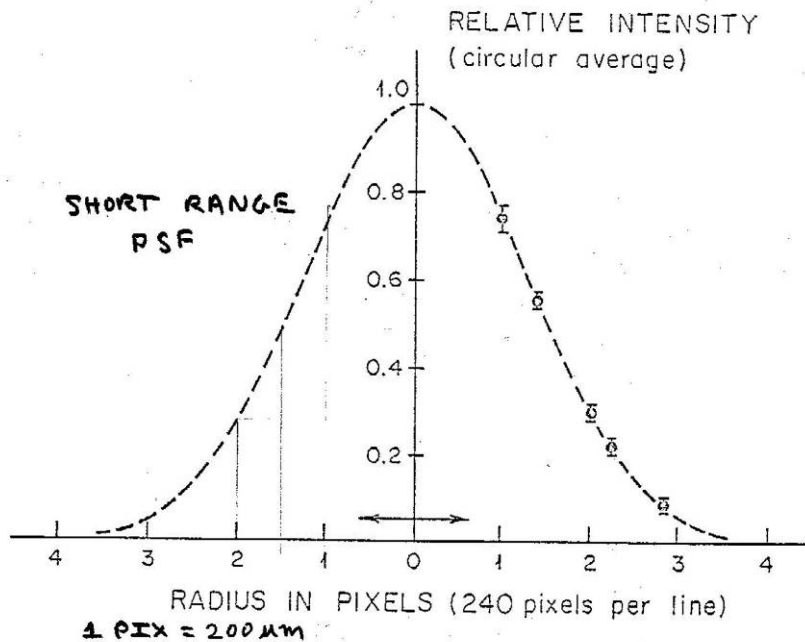
$$MTF(q_x) = \mathfrak{F} [LSF(x)].$$



PSF

Both the short range and the long range PSF are important depending on the problem. The long range PSF requires a physical mechanism for spreading signal around, e.g.,

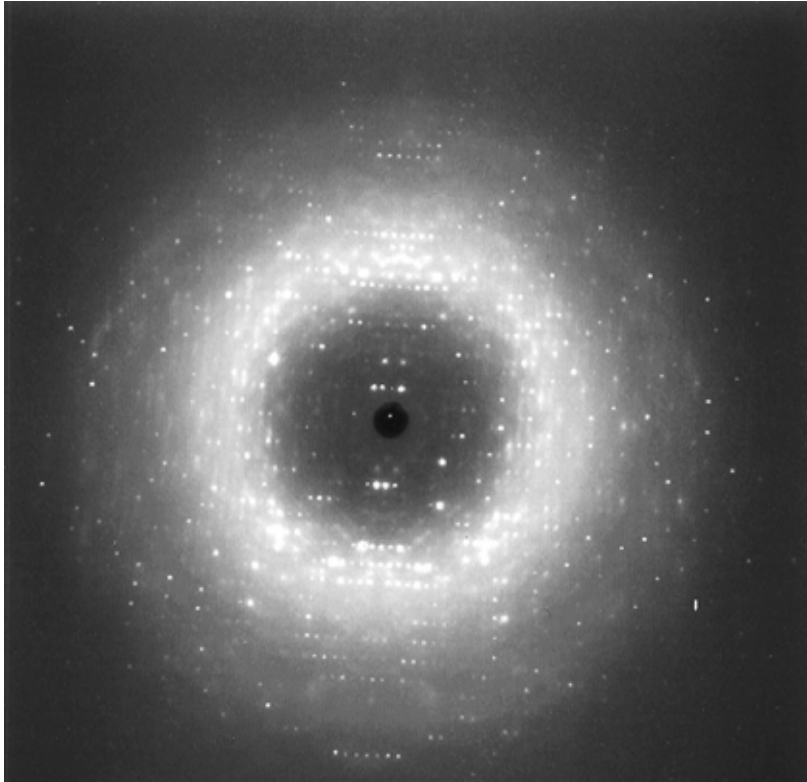
- Light scatter in lens-coupled detectors
- Light scatter in fiber optics with insufficient EMA
- Electron scatter in image intensified detectors.



Short and Long range PSF for a SIT detector. From Gruner et al., Rev Sci Instr 49 (1978) 1241



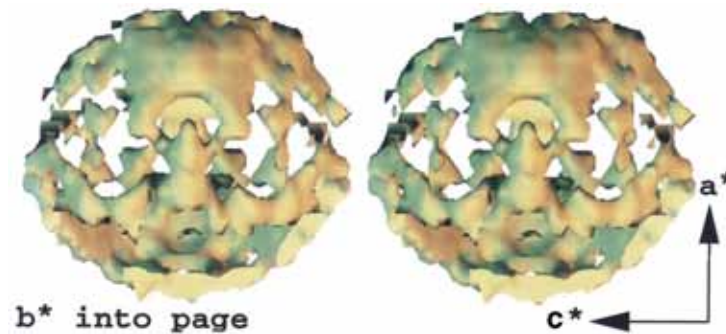
PSF Application Examples



Diffraction of Staphylococcal nuclease crystal.
Wall et al., Proc Natl Acad Sci USA, 94 (1997) 6180.

Long range PSF doesn't hurt: Classical protein crystallography. Bragg spots are locally integrated and a local background measured and subtracted. So bkgnd signal due to long range PSF is subtracted.

Long range PSF is fatal: Analysis of the liquid-like motions of the protein via measurement of the diffuse scatter between Bragg spots. This scatter is 10^{-4} the intensity of the Bragg spots. So long range PSF of the Bragg spots wipes out this very weak scatter.



Stopping Power

Stopping Power = fraction of x-rays stopped in detector recording medium. In low noise detectors,

$$DQE \propto \text{Stopping Power}.$$

Even a noiseless detector with a low stopping power will have a low DQE , because most of the incident x-rays are not recorded. Low stopping power may be suitable for experiments in which there is a strong x-ray signal from a specimen that is not readily damaged by radiation.



Dynamic Range

Unfortunately, there are many definitions of detector **Dynamic Range (DR)**, depending on context. We use:

- Integrating detector:

$$\text{DR} = (\text{sat. signal/pixel})/(\text{zero-dose noise/pixel})$$

for single frame readout.

- Photon counters:

$$\text{DR} = \text{largest signal-to-noise ratio,}$$

i.e., the avg. number of true counts/pixel accumulated before a false count is registered.

In practice, the dynamic range is frequently limited by the readout apparatus or the reproducibility of the detector medium. For example, the large dynamic range of storage phosphors is almost always limited by the capabilities of the reading apparatus, which constrains the saturation signal and limits the zero-dose noise by inability to completely erase the phosphor. The number of bits in the output word does not indicate the dynamic range, since the number of stored bits can only constrain the dynamic range, but, obviously, cannot increase it. Detector manufacturers use ambiguity in the definition of Dynamic Range to horn-swaggle customers.



Dynamic Range

The dynamic range is sometimes given with respect to an integrated signal which spans more than one pixel. For a signal S per pixel which spans M pixels, the integrated signal is MS , and, assuming the noise/pixel, N , adds in quadrature, e.g.,

$$N_{tot.}^2 = \sum_{m=1}^M N^2,$$

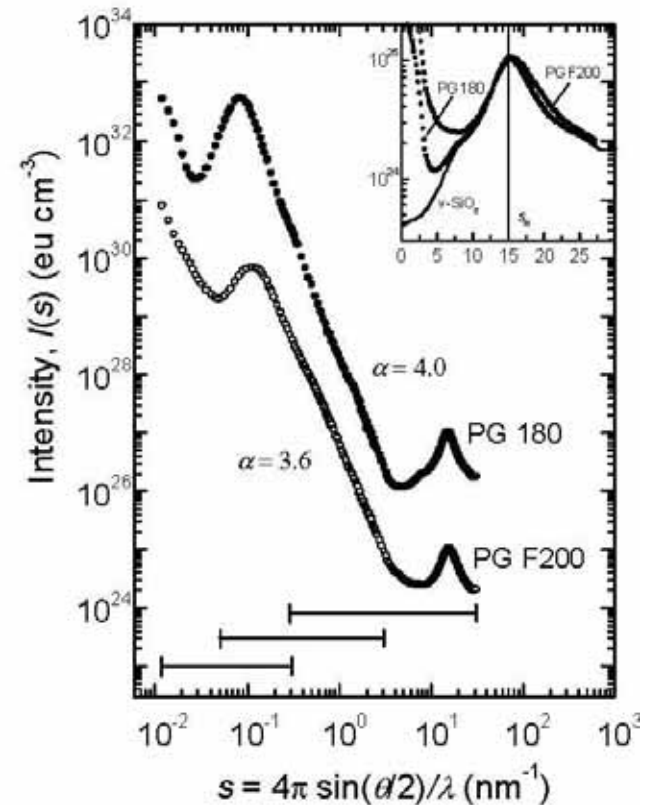
the noise is $N\sqrt{M}$, yielding a factor of \sqrt{M} larger dynamic range. For most detectors, the noise in nearby pixels does not add in quadrature, so this is an upper limit.



“Dynamic Range” is Ambiguous

“Dynamic range” has many meanings; thus, the term is ambiguous.

Consider a Small Angle X-ray Scattering (SAXS) diffraction pattern of Vycor, a porous glass. The data spans many orders of magnitude in intensity. But it would be sufficient to know the accuracy of the data for a given S to only a few percent to do an analysis. In other words, if the curve were given as a list of numbers of intensity, I , versus S , it would be sufficient if I were a floating point number with a 2 digit mantissa and a 2 digit exponent, e.g., 4.6×10^{28} . Here, the dynamic range need be only 100, i.e., at a value of S it is only necessary to know the mantissa to 1%. But the detector should be able to measure intensities (the exponent) over 6 orders of magnitude.



Walter et al., J Appl Cryst 36 (2003) 592.

I advocate using the word **span** to describe the range and **accuracy** to describe the precision to which each number needs to be measured, e.g., The measurement needs to span 6 orders of magnitude in intensity to an accuracy of 1%.



A Detector is only as good as its calibration

Detectors may be compromised by practical considerations of **nonlinearity**, **reproducibility**, and **calibration**. For example, the optical density of x-ray film varies nonlinearly with the incident dose. Although it is possible to calibrate the optical density vs. dose response, in practice, it is difficult to reproduce exactly the film developing conditions required to utilize the highly nonlinear portions of the response. A detector is no better than its practical calibration. This is especially true for area detectors in which the sensitivity varies across the face of the detector. The proper calibration of an area detector is replete with subtleties and constrained by the long-term stability of the calibration. Faulty calibrations are responsible for much of the difference between the possible and actual performance of detectors.

The response of a detector may be nonlinear with respect to position, dose, intensity, and x-ray energy. An x-ray image may also be spatially distorted; this **geometric distortion** can be calibrated if it is stable.



Calibrating to more than 0.5% is VERY hard

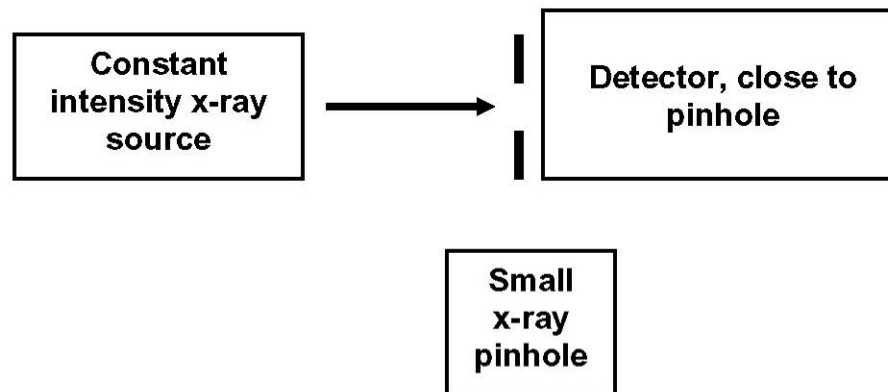
As a practical matter, it is exceedingly difficult to calibrate a detector to better than a few tenths of a per cent.

Claims to the contrary notwithstanding, commercial area detectors are almost never calibrated to better than a percent.

Further, the calibration is dependent on the size of the signal, with very small spots being the least accurate.



Simple Test for Calibration



The following test is useful: Use as small an x-ray opaque pinhole as feasible. Be careful that it is truly of x-ray opaque material. For most detectors, a pinhole in the 25 to 100 micron range is good. Arrange exposure times so the dose through the pinhole is not limited by Poisson statistics to the relevant accuracy, e.g., 10^6 x-rays for a few tenths of a per cent. Verify with a point counting detector, such as sodium iodide/phototube (e.g., Bicron). Measure the integrated dose for random lateral displacements of the detector. Does the standard deviation of the signal correspond to expectations?



Many Practical Considerations...

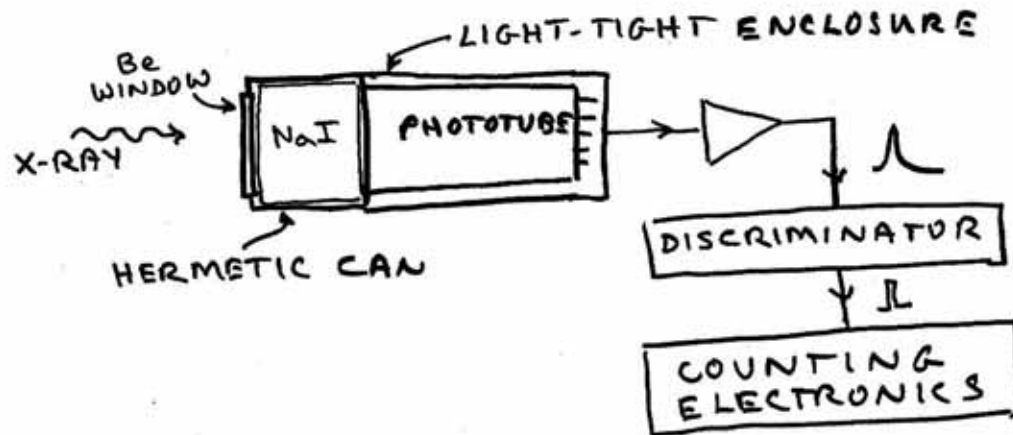
The response of a detector may be nonlinear with respect to position, dose, intensity, and x-ray energy. An x-ray image may also be spatially distorted; this **geometric distortion** can be calibrated if it is stable.

Other detector considerations include the **size** of the detected area and the **format** of the detector (*e.g.*, the number of pixels across the height and width of the detector). The format and the *PSF* limit the number of resolvable Bragg orders across the active area of the detector. **Robustness**: As examples, gas-filled area detectors may be sensitive to vibration of the high-voltage wires; detectors containing image intensifiers are sensitive to magnetic fields; or the detector may simply be easily damaged or lose its calibration during routine handling. Some detectors are readily damaged by too large an x-ray signal. **Count-rate** considerations severely limit the use of many photon counters, especially at synchrotron radiation sources. Detector **speed**, both during exposure and during read out, can be important. Some detector designs are highly **flexible**, permitting special readout modes, such as a selected region of interest for use during alignment, or operation as a streak camera.

Ease of use is important. A detector may simply be hard to use because, for example, it is exceptionally delicate, requires frequent fills of liquid nitrogen, or is physically awkward in size. Another consideration is whether a detector is **well-integrated into an application** with the appropriate analysis software and control software well-interfaced to the other x-ray hardware.



Photon Counters



Scintillator/Phototube Counters

These devices are most suitable as point detectors. Desirable characteristics:

- Scintillator stopping power ≈ 1 .
- Efficient light collection to phototube (reflective enclosures; light coupling grease).
- Rapid scintillations (few μsec).
- Many visible light photons/x-ray (5-25% energy conversion efficiency).
- Robust (e.g., NaI:Tl is hygroscopic; Be enclosures).
- Linear w/resp. to count-rate (10^6 counts/sec).
- Narrow pulse-height distribution (limits energy resolution).

NaI:Tl, CsI:Na, CsI:Tl, BGO (bismuth germanate) are often used as the scintillator..



Physical Properties of Common Inorganic Scintillators

Scintillator	Light Output, % of NaI(Tl) ¹ Bialkali PMT	Wavelength of Max. Emission nm	Decay Time nsec	Half Thickness Value for ¹³⁷ Cs (662 keV) ² cm	Refractive Index ^{3,4}	Density g/cm ³	Hygroscopic	Melting Point °C	Comments
NaI(Tl)	100	415	230	2.5	1.85	3.67	yes	651	Used in many applications; available in a wide range of sizes
CsI(Na)	80-85	430	630	2.0	1.84	4.51	yes	621	High Z; good spectral match to bialkali cathode PMTs; rugged material
CsI(Tl)	45-50	530	1000	2.0	1.80	4.51	slightly	621	High Z; rugged material; good spectral match to PIN diodes and red PMTs
CsI(pure)	4-8	310	~ 8	2.0	1.80	4.51	slightly	621	Fast emission
BGO (Bi ₄ Ge ₃ O ₁₂)	10-20	460	300	1.0	2.15	7.13	no	1050	High Z; low afterglow; high attenuation coefficient
BaF ₂	2* 20	220 325	0.60 630	1.9	1.58 1.50	4.88	slightly ³	1354	Fast component
CaF ₂ (Eu)	50	435	940	2.9	1.44	3.19	no	1418	Low Z; α and β detection; insoluble in most organic solvents
CdWO ₄	30-50	470	15,000	1.0	2.30	7.90	no	1325	High Z; low afterglow; for use with PIN diodes and in detectors for CT/PET scanners
CsF	5	390	5	2.2	1.48	4.11	very	682	High Z; fast emission
ZnS(Ag)	130**	450	70	15 μ stops 5.5 MeV α	2.36	4.09	no	1850	α detection, multicrystal

* Measured with XP2020Q PMT ** Very thin layers *** At wavelength of maximum emission

¹ Ranges are due to geometry differences and material variations. For light output as measured using photodiodes and PMTs with other photocathode types, see references ³ and ⁴.

² Scintillator thickness required to attenuate 1/2 of the incident 662 keV photons; ZnS(Ag) for α only.

³ I. Holl, E. Lorenz, G. Mageras, "A Measurement of the Light Yield of Some Common Inorganic Scintillators", MPI-PAE/Ex.E1.185, October, 1987.

⁴ Sakai, "Recent Measurements on Scintillator-Photodetector Systems", IEEE Transactions on Nuclear Science, Vol. NS-34, Number 1, February, 1987.

⁵ D.F. Anderson, D.C. Lamb, "The Importance of Surface Treatment on the Amount of Light Detected from BaF₂", NIM A260 (1987) 377-380.

FROM BICRON CATALOG



Gas Filled Wire Counters

Gas discharge (wire) counters use the ionization produced when an x-ray is stopped in the high atomic number gas, e.g., Xe. A strong electric field between a fine anode wire and a cathode plane accelerates the products of the primary ionization to produce an ionizing multiplication (either a proportional or an avalanche discharge, depending on the field strength) that is detected as a charge pulse on one or both of the electrodes. The discharge is quenched by the presence of a few percent fraction of a second gas, e.g. methane or carbon dioxide. The venerable Geiger counter is in this class. Properly designed gas discharge counters have very low noise, but the quantum efficiency critically depends on design, gas, and x-ray energy.

Multiwire proportional counters (MWPCs) are 2-D arrangements of crossed planes of wires.

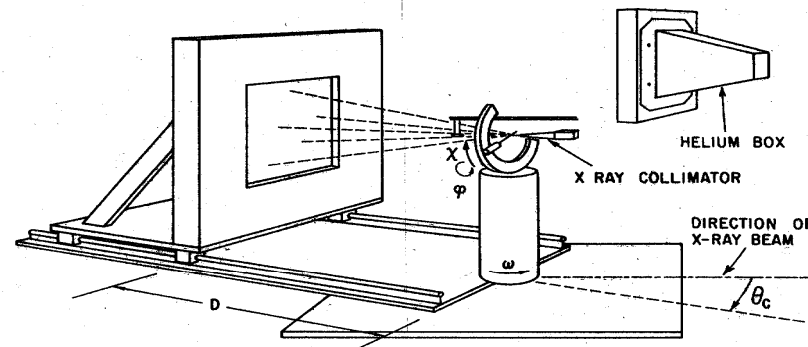


Fig. 4. Crystallographic mounting of the detector. The active surface is shown intercepting several simultaneous diffracted beams (dashed lines) emerging from a crystal mounted on a quarter-circle goniostat. A helium-filled box with mylar front and back windows can be mounted as shown to reduce air scattering of the diffracted beams.

Hamlin et al., *J. Appl. Cryst.* 14 (1981)85



Gas Filled Wire Counters

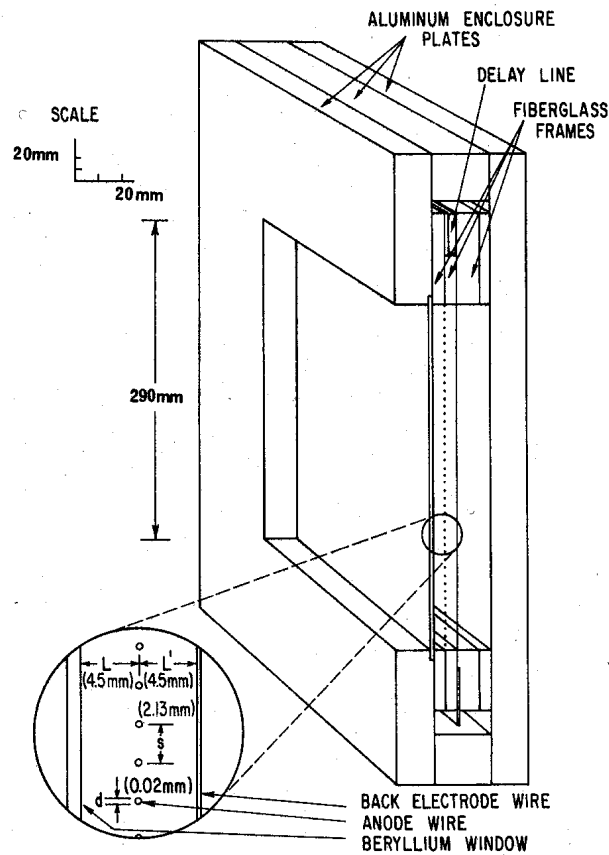


Fig. 1. Cross-sectional view of the detector with detail of electrode spacing.

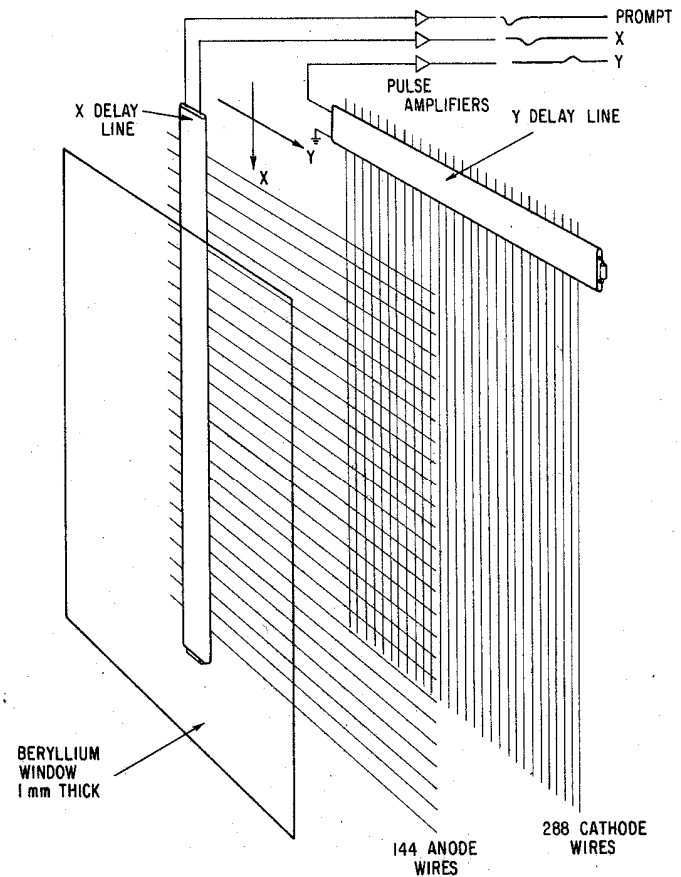


Fig. 2. Relative position of delay lines with respect to the three detector electrode planes (electrode spacing not to scale).

Hamlin et al., *J. Appl. Cryst.* 14 (1981)85



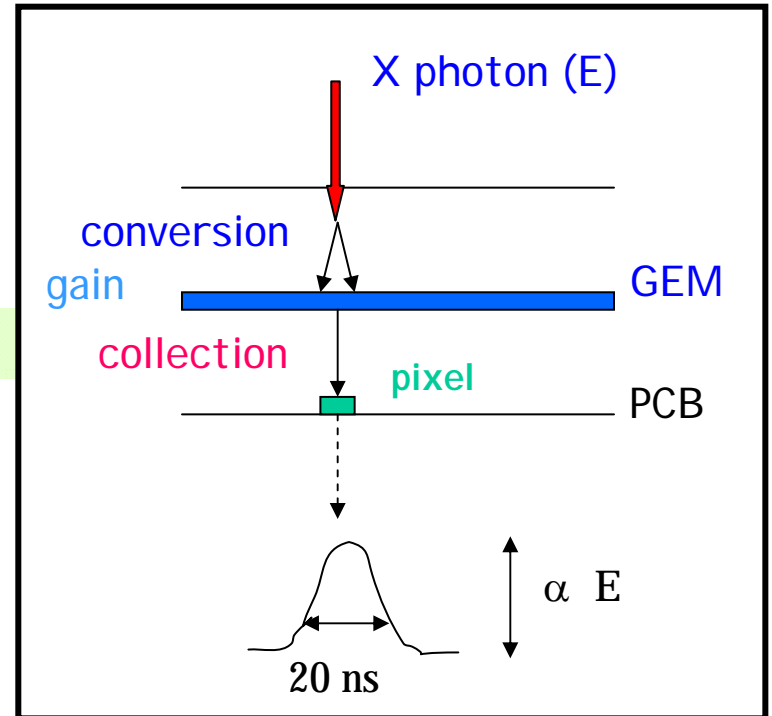
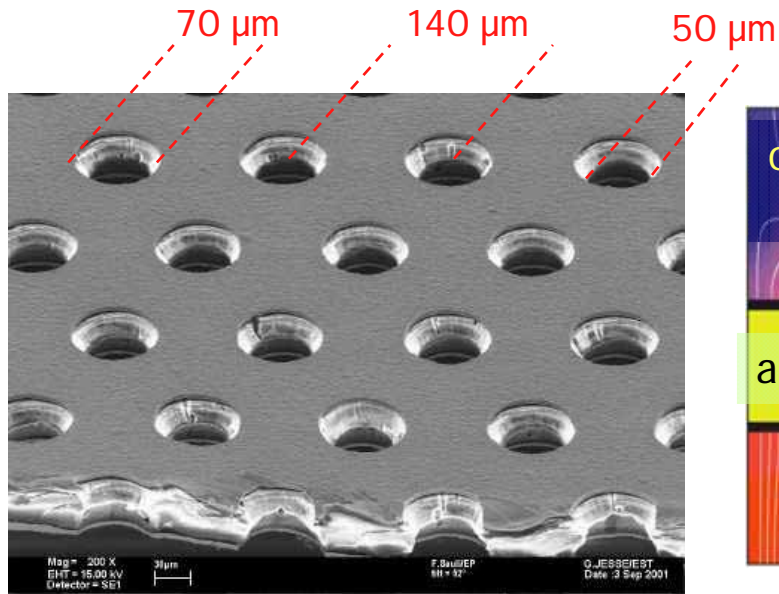
Gas Filled Wire Counters

The design of MWPC area detectors has had difficulty keeping up with improvements in x-ray sources, particularly the high fluxes available at storage rings, and the shift toward use of higher-energy x-rays. The electric discharge at the heart of the technology has an inherent dead time associated with it. Added to this are the pulse propagation and processing times which limit the counting rate for a given wire. Thus, MWPCs are subject to a severe count-rate limitation. A second limitation of MWPCs has been their large pixel size and the relatively small number of pixels across the detector face as well as parallax effects. These problems have been addressed by changes in the detector geometry (*e.g.* spherical drift chambers), by microfabrication on glass substrates of the wires comprising the back plane of the detector, and by dividing the active area into small zones, each of which is read out independently. Robustness of MWPCs has also been a problem.

The dead time can be reduced by reducing the thickness of the detector. However, reducing the detector thickness reduces the x-ray stopping power. Increasing the gas pressure not only improves the quantum efficiency, but also helps to further reduce the dead time. Unfortunately, high gas pressure complicates the design of the front window of the detector. Despite these problems, two-dimensional gas detector prototype modules with 200 μm square pixels have been constructed which are expected to have a local linear count-rate limit of 7 MHz/mm² and a quantum efficiency above 80% at energies used in crystallography.



GEM Detectors



A Gas Electron Multiplier (GEM) (F.Sauli, NIM A386 531 1997) uses $\sim 50 \mu\text{m}$ thick kapton foil, copper clad on each side and perforated by an high surface-density of bi-conical channels.

300 - 500 V across the two copper sides produces an electric field as high as 100 kV/cm. The holes then act as multiplication channels.



GEM Detectors

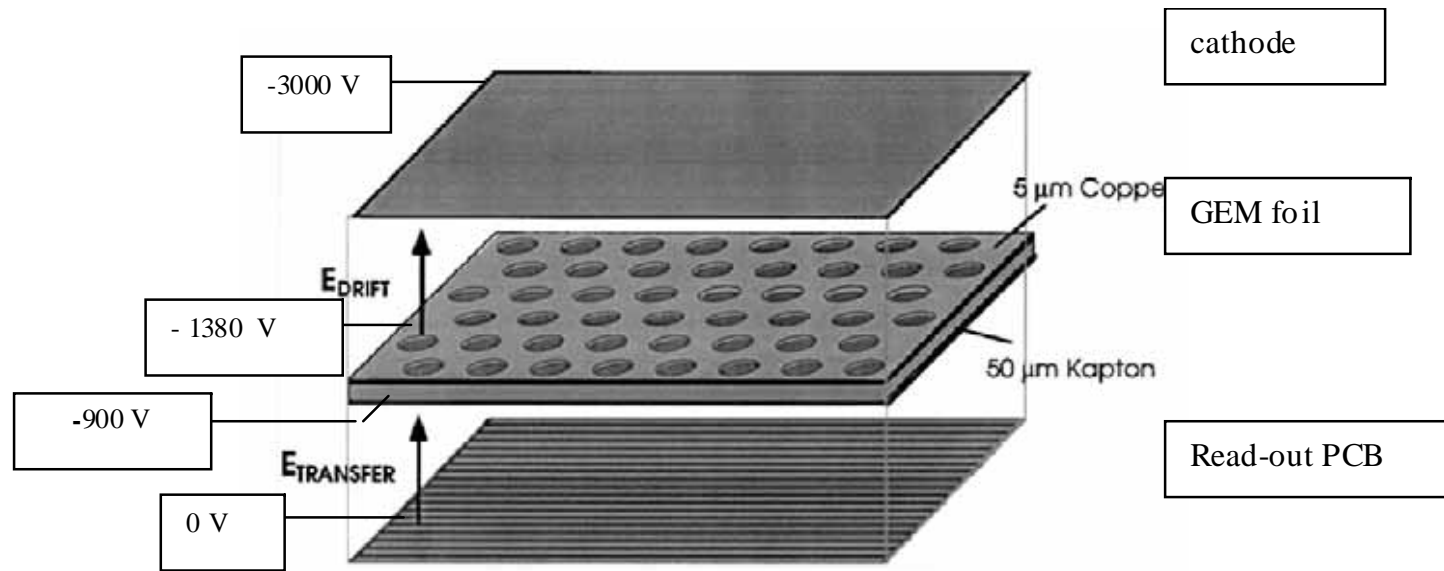


Fig. 19. Schematics of the GEM detector.

